Sensors and Actuators Reports 3 (2021) 100032

Contents lists available at ScienceDirect

Sensors and Actuators Reports

journal homepage: www.elsevier.com/locate/snr

Electrochemical investigations into enzymatic polymerisation of 1,10-phenanthroline-5,6-dione as a redox mediator for lactate sensing

Grace Halpin, Karen Herdman, Eithne Dempsey *

Department of Chemistry, Kathleen Lonsdale Institute for Human Health, Maynooth University, Maynooth Co., Kildare, Ireland

ARTICLE INFO

Keywords:
Lactic acid
Lactate oxidase
1,10-Phenanthroline-5,6-dione
Enzymatic polymerisation
Scanning electrochemical microscopy

ABSTRACT

Lactate biosensor fabrication using a chitosan and crosslinker configuration realised solution mediation ($K_3Fe(CN)_6$) with lactate linear range 9.9×10^{-4} to 5.66×10^{-3} M, sensitivity 1.44×10^{-3}C cm^{-2} mM^{-1} and LOD of 0.54 mM. Further development involved use of the heterocyclic quinoid species 1,10-phenanthroline-5,6-dione which acted as a proton and electron acceptor in relation to $FADH_2$ cofactor regeneration. Graphite ink was formulated and utilised as an underlying conductive layer for LOx enzyme immobilisation and enzymatic polymerisation of 1,10-phenanthroline-5,6-dione at a GC electrode, resulting in a linear range of $0.74 - 2.44\times10^{-3}$ M, sensitivity of 4.11×10^{-4}C cm^{-2} mM^{-1} and LOD of 0.06 mM. Scanning electron and electrochemical scanning microscopy realised surface characterisation of the enzyme layers.

1. Introduction

Lactic acid detection and quantification is important in various areas of healthcare and sports nutrition [1]. It is normally measured in serum samples for diagnosis and medical management of a wide range of different medical issues including hyperlactatemia, sepsis, lactic acidosis and hypoxia-induced cancer [2]. Many lactic acid biosensors have been previously designed for serum sample analysis to enable rapid diagnosis of medical concerns. Use of enzymatic biosensors for clinical diagnosis are favourable due to their low cost, specificity and sensitivity. Generally, they are based on lactate oxidase (LOx) or lactate dehydrogenase (LDH) immobilisation on a transducer surface [3,4]. LOx is a globular flavoprotein most commonly derived from a variety of microorganisms, including *Pediococcus* species and *Aerococcus viridians* [5]. LOx is also more commonly used due to the enzyme reaction involving production of H_2O_2. When the hydrogen peroxide is then oxidised at the surface, the initial oxygen concentration is regained and the measure of current is proportional to the amount of lactate present in the sample matrix [6]. Development of a lactate reagent-less biosensor has been carried out recently by Bravo et al. for determination of lactate in food samples [5]. Investigations into the development of a bi-enzyme amperometric graphite biosensor for the determination of lactic acid was carried out by Herrero et al. [7]. This was achieved by immobilisation of Horseradish Peroxidase (HRP), LOx and ferrocene onto a Graphite-Teflon sensor to determine lactate in yoghurt products. A bienzyme amperometric graphite-Teflon composite biosensor was used for lactic acid quantification in cow milk, goat milk and whey protein concentrates (WPC) [8]. This system combined the use of ferrocene as a mediator with enzymes horse-radish peroxidase (HRP) and L-lactate oxidase (L-LOD).

Electron transfer mediators include ortho-quinoidal compounds, which have been of interest in electrochemical biosensors due to their chemical stability, electrochemical reversibility, ideal equilibrium potential and their high reactivity towards redox-active enzymes [9]. In the case of glucose oxidase (GOx) sensors, quinones are reduced by a two-electron (hydride) transfer reaction involving an electron transfer mechanism that is governed by electron-accepting forces of the compounds without hindering their chemical properties [9]. Ortho-quinoidal compounds are favourable for GOx mediated systems due to the high self-exchange rate constants of quinones combined with their high rate of reaction with the reduced form of GOx and the electrode surface [9,10].

1,10-Phenanthroline is the primary compound of a class of chelating agents which together form a large number of chemical compounds with different metal complexes. These complexes have previously been studied for their ability to act as redox indicators for quantitative analysis given their high redox potential [11]. Studies have shown how these compounds can be used as redox mediators for oxidases and can enable fabrication of reagent-less biosensors when electrodeposited or polymerised onto a transducer surface [12]. This work focuses on 1,10-Phenanthroline-5,6-dione (PD) and its ability to act as a redox mediator in lactate biosensing. PD a versatile ortho-quinoidal compound that contains two diiminic nitrogen atoms that allow metal ion binding and the *o*-quinoid part of the molecule that is responsible for redox activity. PD along with another ortho-quinoidal compound 9,10-Phenanthrenequinone (PQ) were used in a study to investigate their use as mediators in

* Corresponding author.
E-mail address: eithne.dempsey@mu.ie (E. Dempsey).

https://doi.org/10.1016/j.snr.2021.100032
Received 11 December 2020; Revised 7 February 2021; Accepted 9 February 2021
Available online 13 February 2021

amperometric graphite rod electrodes modified with GOx [9]. The two electrodes were prepared by depositing 3 μL of either PD or PQ onto the surface of a graphite rod electrode three times before enzyme modification with GOx. During the reaction, quinone was reduced to hydroquinone in the presence of the reduced enzyme GOx and was re-oxidised by the heterogeneous electrode reaction [10]. It was shown that PD was a more efficient mediator for use in biosensors compared to PQ with current response seven times higher than that of the PQ-modified sensor. It was suggested this may be due to the presence of azomethane moieties on the PD structure which can enable higher electron (hydride)-accepting potency and therefore faster electron transfer rate [9] The reactivity of both mediators was also assessed using a model single electron transfer FAD-dependant enzyme, $NADP^+$ ferredoxin reductase, which showed that PD had a higher reactivity than PQ [9]. Investigations have also been performed that involve the use of Osmium Phenanthroline compounds such as Os(4,4′-dimethyl, 2,2′-bipyridine)$_2$(1,10-Phenanthroline-5,6-dione) in the development of reagentless dehydrogenase carbon paste amperometric electrodes for glucose detection, where the alternative enzyme GDH was used [13].

Recent studies have shown how PD can be used for the development of thin-film glucose biosensors, via enzymatically synthesised poly(1,10-Phenanthroline-5,6-dione) (pPD) in the presence of the enzyme, GOx [14]. This technique allowed the encapsulation of the GOx enzyme within a polymer film that was formed during the production of H_2O_2. The pPD/GOx film was prepared by submerging a GOx-modified graphite rod electrode in a buffer solution containing both the enzyme substrate, glucose (25 mM), and the mediator, PD (5 mM) for 24 hrs at 4 °C. The generation of H_2O_2 during catalysis initiated polymer synthesis which caused a biocompatible "shell" to form over the now embedded enzyme [14]. Previous studies involving biocompatible enzymatic-inks were used for direct detection of glucose [15] and exploited graphite inks to enable "on-demand" and "on-site" fabrication of enzymatic sensors that could cater to specific needs of the user. Using the graphite ink, enzymatic roller pens were designed which demonstrated good reproducibility and the ability to draw bio-catalytic conducting traces on a wide range of surfaces.

Scanning electrochemical microscopy (SECM) is an electrochemical tool used to probe surfaces and analyse surface reactions by using a scanning probe technique [16]. The basis of SECM involves the use of an ultramicroelectrode (UME) tip which has been described as an electrode with a radius usually 25 μm in size. SECM measures the current that passes through the UME while it is held stationary or moving through an electrolyte solution surrounding the substrate. The main applications of SECM are to analyse both heterogenous and homogenous electrochemical reactions and as an imaging tool to analyse the topography of different material surfaces [17]. Redox competition mode (RC-SECM), was described by Morkvenaite-Vilkonciene et al. for its use in evaluation of enzyme kinetics in GOx immobilised electrodes [18]. It involves the UME and the sample competing for the same analyte in the bulk solution. The current for oxygen reduction is generally held constant throughout the experiment unless the UME is within the area of oxygen consumption which can be measured at a bipotentiostatic mode involving the UME and the substrate electrode held at the potential for oxygen reduction [19]. It is often used to investigate local catalytic activity of immobilised enzymes on the surface of electrodes by evaluation of oxygen reduction reactions. This is performed by both the immobilised enzyme and the UME competing for dissolved O_2 [19]. When higher concentrations of glucose are present, the concentration of oxygen at the surface of the enzyme modified surface decreases as it is used up in the enzymatic reaction. Along with horizontal scanning methods, RC-SECM can be used for the analysis of enzyme electrode substrates where the redox mediator can be involved in two simultaneous processes including the electron uptake with the enzyme and recycling of the mediator to its oxidation state at the conducting surface.

The research involved first time deposition (via enzymatic polymerisation) of an ortho-quinoidal compound, 1,10-Phenanthroline-5,6-dione, onto a LOx enzyme layer with electrochemical and surface characterisation. An underlying graphite ink layer provided a biocompatible environment for protein stabilisation with the PD film acting as a stable redox active layer for lactate mediation with improved analytical performance. To date, there has been no evidence for such an approach in lactate sensor development.

2. Experimental

2.1. Materials

Poly(ethylene glycol), Chitosan, Xylitol, 1,10-Phenanthroline 5,6-dione, potassium phosphate dibasic anhydrous, potassium dihydrogen phosphate, Lactate Oxidase from Aerococcus viridans, Glutaraldehyde (GA), Poly(ethylene glycol) diglycidyl ether (PEGDE), Bovine serum albumin, graphite powder and Sodium L-lactate standard were all purchased from Sigma Aldrich. Acetic acid was purchased from AppliChem Panreac, an ITW company.

2.2. Instrumentation

All electrochemical techniques were carried out on a Solartron 1285 potentiostat with electrochemical software CorrWare and CorrView for data analysis. A three-electrode cell utilised Pt wire as counter electrode, a Ag/AgCl reference electrode (stored in 3 M KCl) and either platinum (Pt), glassy carbon (GC) or screen printed carbon electrode (SPE) as working electrode. Macro electrodes were polished using 1 μm MetaDi Monocrystalline Diamond suspension followed by rinsing in deionised water and sonication to remove any residual polishing agent. Scanning Electron Microscopy with Energy Dispersive X Ray spectroscopy was performed on a Hitachi with Au/Pd sputter coater. Scanning Electrochemical microscope M380 Biologics instrument with Isoplot image software (3D plots).

2.3. Procedures

2.3.1. Preparation of graphite ink

The preparation of graphite ink solution (GInk) was adapted from that described by Bandodkar et al. [15]. The binders PEG (60% in dH_2O) and chitosan (1% in 0.1 M acetic acid) were mixed in a 2:1 ratio in the presence of the stabiliser xylitol (2 M in dH_2O), followed by addition of graphite powder to give 40% w/v. The so-prepared ink was stirred for 10 min before sonication for 30 min (to ensure dispersion) and stored at 4 °C. The ink underwent both surface (SEM/EDX) and electrochemical characterisation.

2.3.2. Preparation of lactate oxidase electrodes

A four-layer reagent system consisting of (a) 5 μL of a 0.5% chitosan in 0.8% acetic acid (b) 5 μL of enzyme mixture (4 U LOx for lactate detection in the presence of 0.5 mg mL^{-1} BSA in 0.02 M phosphate buffer (PB) pH 6.0)) (c) repeat of step (a) (d) 5 μL of 1.5% GA (or PEGDE in the case of the glassy carbon electrode for 1,10-Phenanthroline-5,6-dione modification). Each layer was allowed to dry at room temperature between modification steps. Electrodes used were labelled GC/Chit/LOx/Chit/GA (or Pt/Chit/LOx/Chit/GA where the Pt transducer allowed confirmation of direct detection of hydrogen peroxide in response to lactate substrate SI(1)).

Solution phase mediated sensing was performed via CV at modified GC electrodes (GC/Chit/LOx/Chit/GA) with Lactate (0–7 mM) in the presence of 5 mM $K_3Fe(CN)_6$ over the potential range −0.5 V to 0.7 V vs. Ag/AgCl at 20 mVs^{-1}. Lactate calibration (0–12 mM) was carried

out via chronocoulometric analysis with E_{app} = 0.38 V vs. Ag/AgCl for 5 s.

Graphite ink modified electrodes involved drop casting 1 μL of GInk onto the GCE surface which was allowed to dry at room temperature for 10 min. This was followed by LOx immobilisation as described above with step (d) 1.5% PEGDE. Electrodes are referred to as GCE/LOx or GCE/GInk/LOx.

2.3.3. Poly(1,10-phenanthroline-5,6-dione) film formation at LOx modified GCE

Polymerisation of 1,10-Phenanthroline-5,6-dione involved sequential additions of lactate during potential cycling in the presence of PD (5 mM) and lactate additions (1−4 mM) at GCE/LOx electrode over the potential range −0.8 V to 0.8 V vs. Ag/AgCl at 20 mVs^{-1}. Stabilisation of the film was performed by cycling the electrode in 0.1 M phosphate buffer (pH 4.0 and 6.0) over the potential range −0.8 V to 0.8 V vs. Ag/AgCl at 100 mVs^{-1}. 5 mM PD (in 0.1 M phosphate buffer (PB) (pH 6.0) was prepared by sonication (5 min). PD deposition via enzymatic polymerisation was performed at modified electrodes (GCE/GInk/LOx or GCE/LOx) at 20 mVs^{-1} over the potential range −0.7 V to 0.7 V vs. Ag/AgCl. Lactate additions followed with CV recorded (under the same conditions) between each addition until a final concentration of 4.76 mM lactate was reached. The electrode was rinsed with buffer prior to electrochemical analysis and film studies. All electrodes modified with pPD films (see Scheme 1) are labelled GCE/LOx/pPD or GCE/GInk/LOx/pPD.

2.3.4. Electrochemical film studies of poly(1,10-phenanthroline-5,6-dione)

Film stability studies involved electrode cycling in 0.1 M PB (pH 6.0) at modified electrodes for 20 cycles at 100 mVs^{-1}. Scan rate studies were performed over the relevant ranges in the same electrolyte.

2.3.5. Detection of L-lactate at poly(1,10-phenanthroline-5,6-dione) modified graphite ink electrodes

The response to lactate at GCE/GInk/LOx/pPD electrode was examined using CV at 100 mVs^{-1} over the range −0.7 V to 0.7 V vs. Ag/AgCl. Chronocoulometry (CC) analysis was performed at (E_{app} = −0.12 V or 0.12 V vs. Ag/AgCl) to enable monitoring of the lactate response at cathodic/anodic pPD peak potentials respectively.

2.3.6. Surface characterisation of lactate biosensor using scanning electrochemical microscopy

Solution phase mediated sensing was performed via CV at modified GC electrodes (GC/Chit/LOx/Chit/GA) with Lactate (0−7 mM) in the presence of 5 mM $K_3Fe(CN)_6$ over the potential range −0.5 V to 0.7 V vs. Ag/AgCl at 20 mVs^{-1}. Approach curves were carried out in 5 mM

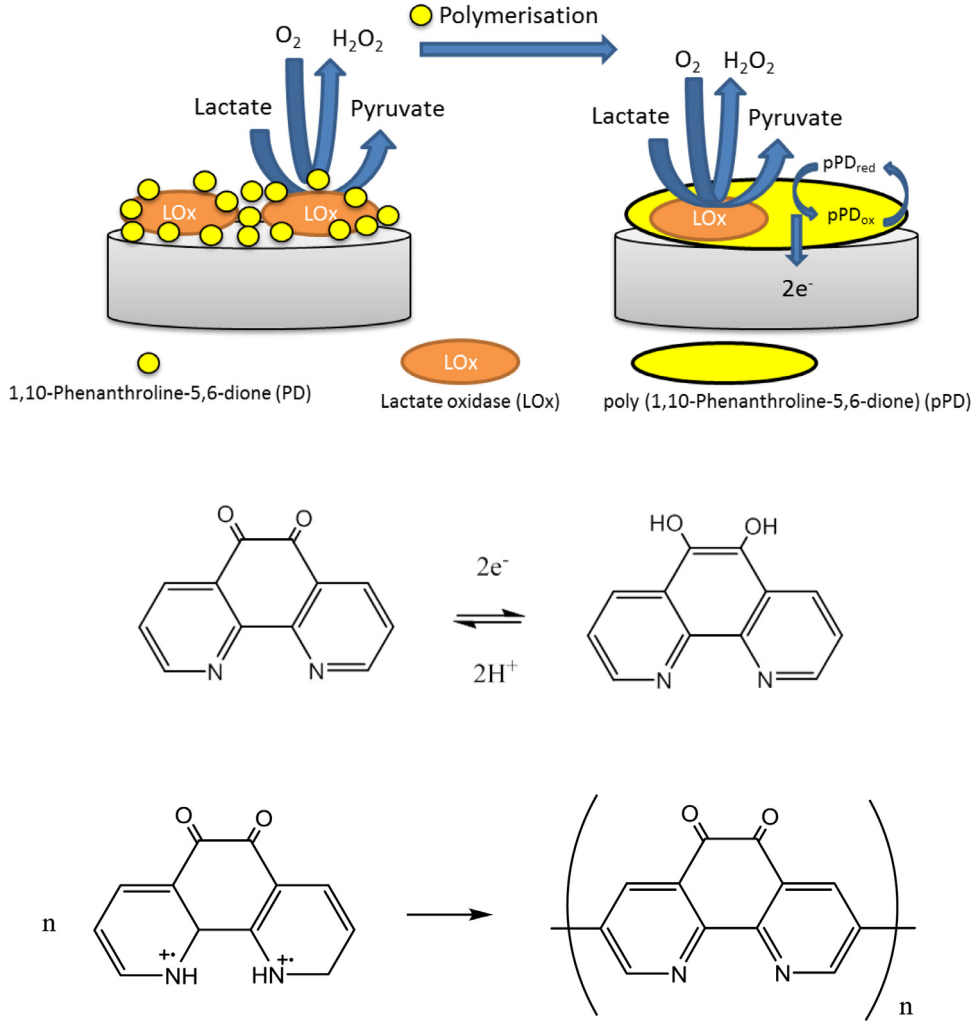

Scheme 1. (Top) Schematic of 1,10-Phenanthroline-5,6-dione deposition via enzymatic polymerisation at LOx modified electrode, in the presence of enzyme substrate and *in situ* generated H_2O_2 oxidant. (Below) Redox process for 1,10-Phenanthroline-5,6-dione and polymer formation.

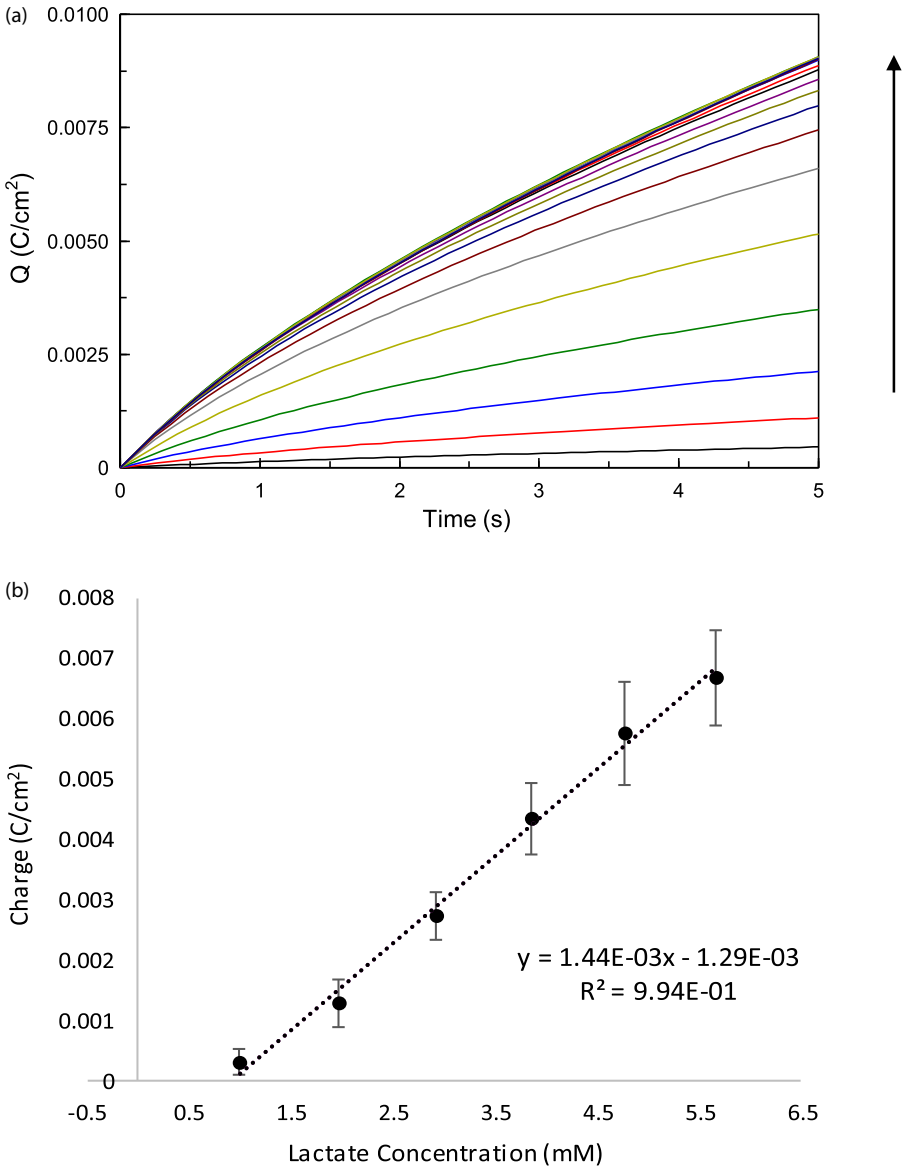

Fig. 1. (a) Overlay of chronocoulometry data 0–12 mM Lactate concentrations at a GC/Chit/LOx/Chit/GA electrode in the presence of 5 mM $K_3Fe(CN)_6$ (E_{app} = 0.38 V vs. Ag/AgCl for 5 s). (b) Corresponding data plot of charge vs. concentration (0.99 - 6 mM Lactate) in 5 mM $K_3Fe(CN)_6$ (n = 3).

$K_3Fe(CN)_6$ using a Pt UME tip with the tip potential (E_T) held at −0.4 V vs. Ag/AgCl (E_{sub} = OFF). The movement of the tip to the surface of the substrate (enzyme modified GC electrode) was monitored and stopped prior to contact. Redox competition mode was utilised where both sample and tip compete for Fe^{3+}. High local electroactivity was indicated by low currents monitored at SECM tip as enzyme modified surface was approached. Line scans were carried out by measuring the current at −0.4 V vs. Ag/AgCl as it scanned across the electrode surface (0 - 8000 mm) in 5 mM $K_3Fe(CN)_6$ and in the presence of lactic acid (20 mM). Imaging of the enzyme layer was achieved via area scans of the modified substrate electrode to examine the area of enzyme activity with (E_T = −0.4 V vs. Ag/AgCl E_{sub} = OFF) 5000×5500 mm^2 with 100 mm^2 per point. Scans were carried out in 5 mM $K_3Fe(CN)_6$ with 0 or 20 mM substrate.

3. Results and discussion

3.1. Solution phase mediation studies

Voltammetry was used to evaluate the lactate response (0–7 mM) at a GCE/Chit/LOx/Chit/GA electrode in the presence of 5 mM $K_3Fe(CN)_6$ with a linear increase in response evident at 0.3 V vs. Ag/AgCl (SI(2)). Further electrochemical analysis was carried out via chronocoulometry with E_{app} = 0.3 V vs. Ag/AgCl for 5 s (Fig. 1(a)) with increasing lactate (0–12 mM)). Fig. 1(b) shows the corresponding calibration curve resulting in a linear range of 0.99 - 6 mM, sensitivity of 1.44×10^{-3}C $cm^{-2}mM^{-1}$, LOD of 1.19 mM and LOQ of 3.97 mM. There was an initial lag in sensor response to lactate additions which may be due to oxygen interference.

Scanning electrochemical microscopy was employed to examine these enzyme layers in the presence of mediator in solution providing surface topographical and imaging/enzyme reactivity information. Approach curves were carried out in 5 mM $K_3Fe(CN)_6$ with the UME tip potential (E_T) held at −0.4 V vs. Ag/AgCl (E_{sub} = OFF). The movement of the tip to the surface of the substrate (enzyme modified GC electrode) was monitored and stopped prior to contact. Redox competition mode was utilised (Scheme 2) – where both sample and tip compete for Fe^{3+}. High local electroactivity was indicated by lowered nA current signals monitored at the SECM tip as the enzyme modified surface was approached. Approach curves and line scans confirmed the enzymatic catalytic response in the presence and absence of enzyme substrate in the presence of $K_3Fe(CN)_6$.

Fig. 2(a) shows an approach curve towards the enzymatic LOx biosensor substrates (E_T = −0.4 V vs. Ag/AgCl). As the tip approached the

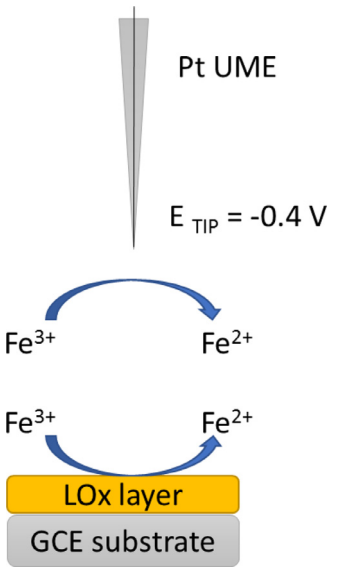

Scheme 2. Redox competition mode for Fe^{3+} using scanning electrochemical microscopy at LOx modified GCE (E_T = −0.4 V vs. Ag/AgCl) E_{sub} = OFF, 20 μm Pt UME (RG = 23.8).

LOx modified surface, the current decreased causing a negative feedback response. A sharp decrease in current was evident upon approach to the modified electrode and the experiment was stopped at this point. Redox competition mode was used where both the tip and modified substrate electrode competed for Fe^{3+} ions in solution. High local electroactivity was reflected in low current being measured at the SECM tip upon approach to the enzyme modified surface. A series of approach curves were performed at the LOx electrode with varying concentrations of $K_3Fe(CN)_6$. Fig. 2(b) shows approach curves to the LOx electrode in 0.1 − 2 mM $K_3Fe(CN)_6$ where current was measured at E_T = 0.4 V vs. Ag/AgCl showing the relationship between tip current and the concentration of $K_3Fe(CN)_6$. Here, an increase in $K_3Fe(CN)_6$ concentration caused lower current due to the negative feedback response.

Line scan studies were performed in the presence of 0 and 20 mM lactate in 5 mM $K_3Fe(CN)_6$) in order to demonstrate that the current detected was responsive to substrate concentration. Fig. 2(c) shows the change in current value upon scanning across the substrate electrode surface (0–8000 μm). Results showed that in the absence of lactate, no change in current was detected as no regeneration of electroactive species occurred. When 20 mM lactate was added, there was a fluctuation in current as the tip moved across the enzyme modified electrode surface and current increased again once past the enzyme modified region. The enzyme loaded regions beyond the conducting disk may contribute to the 1 nA baseline difference evident either side of the minimum observed in the most active region.

Area scans were carried out on the enzyme modified electrode using 5 mM $K_3Fe(CN)_6$ as an electron transfer mediator where the tip potential was held constant (E_T = −0.4 V vs. Ag/AgCl) which causes reduction of Fe^{3+} to Fe^{2+}. An approach curve was performed at the GCE/Chit/LOx/Chit/GA in order to determine the appropriate position of the tip over the substrate (modified electrode) in the electroactive region. Fig. 3 shows area scan experiments at a GCE/Chit/LOx/Chit/GA electrode with 5 mM $K_3Fe(CN)_6$ in the absence (0 mM) and presence of lactate (20 mM). Results showed that in the presence of substrate (20 mM), the current signal decreased at the enzyme modified region of the electrode surface. Therefore, the active region of the LOx modified surface could be visualised by observation of a dark blue circular feature at the current minimum. The presence of LOx caused regeneration of Fe^{2+} as the UME tip competes for Fe^{2+} reduction, therefore it was possible to visualise the region where LOx was catalytically active.

3.2. Electrochemical growth and characterisation of 1,10-phenanthroline-5,6-dione film on GCE/LOx

The use of 1,10-Phenanthroline-5,6-dione (PD) was investigated for its use as an electron transfer mediator in lactate biosensing. Electrodes were prepared using a layer-by-layer system of chitosan/LOx/chitosan/PEGDE (as per Section 2.3) and will be referred to as GCE/LOx or GCE/LOx/pPD after electrochemical polymerisation of the mediator onto the modified electrode. Figure 9. The approach taken for enzymatic polymerisation involved increasing lactate additions (1 − 4.76 mM) at scan rates of 20 mVs^{-1}. Fig. 4 shows the decrease in PD reduction peak as the concentration of lactate increased in the cell. There was a slight increase in the oxidation peak during growth. Following PD deposition, a bright thin yellow film was evident on the electrode surface.

Following film stabilisation by cycling in phosphate buffer, a scan rate study was performed at the GCE/LOx/pPD (2–300 mVs^{-1}) (Fig. 5). At slower scan rates (2 mVs^{-1}), the oxidation and reduction peaks appeared to superimpose over each other and were symmetric, characteristic of an ideal reversible surface confined voltammogram. Plots of (a) I_{pa} and I_{pc} vs. ν and (b) $\sqrt{\nu}$ resulted in a linear trend being observed (<50 mV/s) in the case of *(a)* indicating surface confined thin film behaviour for the redox process (SI(3)).% decrease in activity upon cycling was 6.64% and 2% for the anodic and cathodic waves respectively (over 20 cycles).

Electrochemical and surface characterisation of graphite ink was performed for examination as an underlying layer in the enzymatic pPD film formation. Voltammetry and chronoamperometry was carried out on the graphite ink (GInk) modified GCE prior to enzyme immobilisation in order to determine the surface area of the electrode and to calculate the capacitance of the ink layer (see SI(4)) as 9.22 mF cm^{-2}. Scanning electron microscopy (SEM) images were taken of both a commercial bare carbon screen printed electrode (SPE) and a modified SPE/GInk/LOx/pPD. Fig. 6 shows SEM images of a bare SPE *(a)* and a modified SPE (SPE/GInk/LOx/pPD) *(b)* with rod-like structures appearing on the surface of the latter surface. The structures varied greatly in width and length with average measuring at 6.47 μM and were very uniformly distributed across the surface of the electrode. Energy Dispersive X-ray (EDX) analysis was also carried out on the surface of a bare SPE and modified SPE (SPE/GInk/LOx/pPD) (SI(5)).

Fig. 7 shows a voltammogram representing pPD film formation onto a GCE/GInk/LOx electrode. A decrease in the reduction peak at 0.1 V was evident as the concentration of sodium lactate increased in the electrochemical cell. After film formation, the working electrode was rinsed with deionised water. The appearance of the GCE/GInk/LOx/pPD showed as a thin bright yellow film as before, indicating the successful polymerisation of pPD.

Film studies (Fig. 8) resulted in minimal reduction in the peak current for both oxidation and reduction peaks after 20 cycles at 100 mV s^{-1}. Results showed that using the graphite ink as the underlying layer, allows a better quality thin film to be achieved, with more defined oxidation and reduction peaks (surface coverage 5.3 × 10^{-9} mol/cm^2). There was also evidence of improved electrochemical reversibility of the polymer, which may be due to interactions between the conducting ink layer and the PD film. Intermolecular self-complexation of PD with its reduced form (via H bonding between the pyridine N atoms and the hydroxy groups of the reduced form) results in a diol which is insoluble and can impede re-oxidation [20]. The addition of the graphite ink as the underlying layer results in more efficient and reversible electron transfer, with π–π and hydrophobic surface interactions influencing this diol formation as shown previously with an underlying carbon nanotube layer [20]. In the absence of GIink, pPD films exhibited ΔEp 0.109 V with $E_{1/2}$ −0.015 V, while with the GInk underlying layer ΔEp decreased to 0.072 V with a slight cathodic shift in $E_{1/2}$ to −0.027 V (pH 6 and 20 mV/s in both cases).

A shift in peak potential was evident when the film was examined in more acidic conditions, with the redox film demonstrating

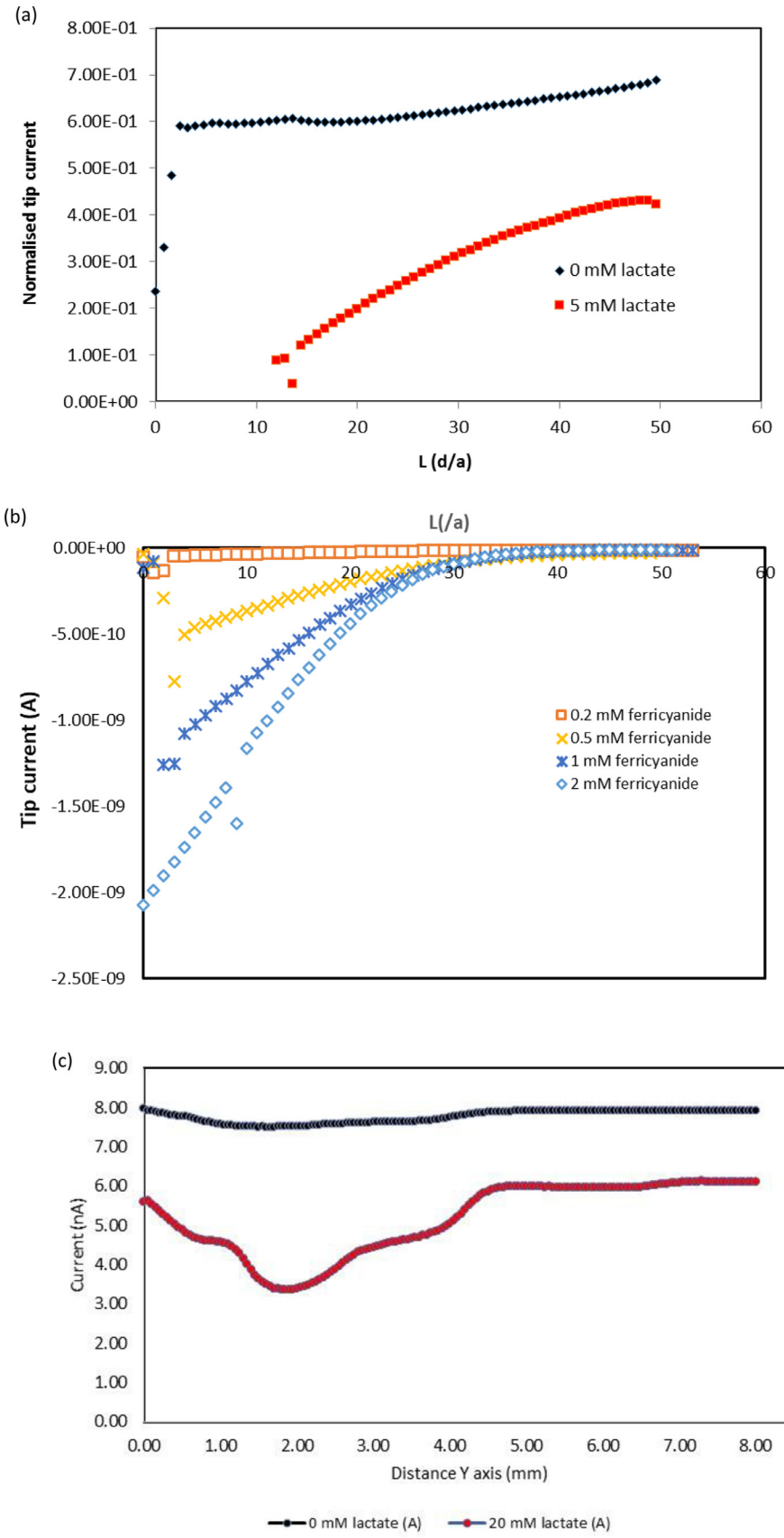

Fig. 2. (a) Normalised current (I_{TIP}/I_{Inf}) vs. distance (L) where $L = d/a$ and d = distance from tip Pt ultramicroelectrode (UME) to substrate, a = tip radius 20 μm, RG = 23.8. Curves recorded above the Chit/GA-LOx film, by translating the UME vertically (z approach curve). E_T = −0.4 V vs. Ag/AgCl, E_{sub} = OFF, 5 mM $K_3Fe(CN)_6$ in PB pH 6.0. (b) Approach curves to LOx sensor in various mediator concentrations in the presence of 15 mM lactate (E_T = 0.4 V) SGTC mode (c) Line scan (Y direction) across LOx modified electrode E_T = −0.4 V vs. Ag/AgCl, E_{sub} = OFF, Scan range 8000 mm, 50 mm/point in 5 mM $K_3Fe(CN)_6$.

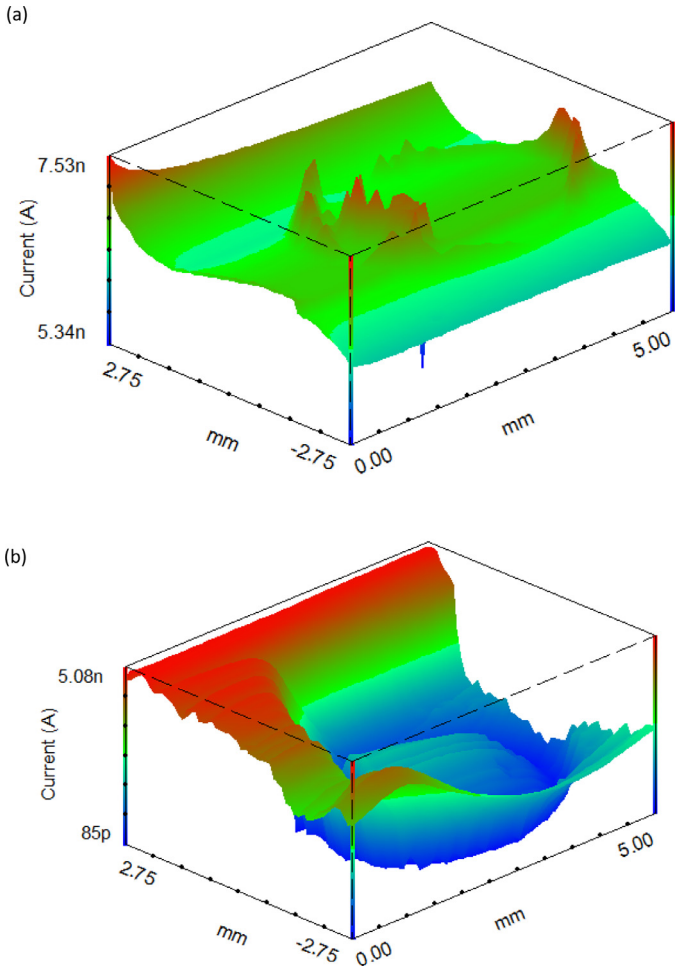

Fig. 3. Area scan SECM experiment at E_T = −0.4 V vs. Ag/AgCl E_{sub} = OFF, (20 μm Pt, RG = 23.8) 5000×5000 mm^2 100 mm per point at LOx modified GCE substrate in 0 mM (a and b) 20 mM lactate in the presence of 5 mM $K_3Fe(CN)_6$.

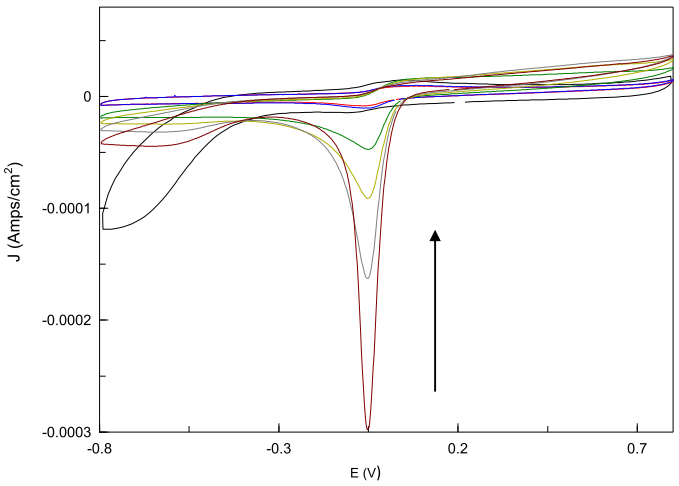

Fig. 4. CV showing additions of lactate (1−4.76 mM) to a solution of 5 mM PD in 0.1 M PB (pH 6.0), at a GCE/LOx with enzymatic polymerisation resulting in pPD formation. Potential range −0.8 V to 0.8 V vs. Ag/AgCl at 20 mVs^{-1}. Cathodic peak at −0.1 V decreases upon lactate additions (first addition — 1 mM lactate).

$E_{1/2}$ = 0.0284 V for the pH 6 environment and $E_{1/2}$ = 0.0854 V in a pH 4 environment, confirming the pH dependant process (2e$^-$ 2H$^+$). An additional redox process was evident at −0.3 V in pH 4 buffer, indicating that the polymer may undergo further reduction processes, possibly step wise reduction via the N protonated hydroquinone form which may be influenced by the surface graphitic layer.

The modified electrode was then examined in relation to its analytical performance using both CV and CC. Fig. 9 (a) shows a CV in background electrolyte and 0.99 mM sodium lactate with response to lactate evident at 0.1 V indicating oxidation of pPD as I_{pa} increases and I_{pc} decreases at −0.1 V following reduction of the mediator.

$$Lactate + LOx(FAD) \rightarrow Pyruvate + LOx(FADH_2)$$

$$LOx(FADH_2) + +PD(_{OX)} \rightarrow LOx(FAD) + H_2PD_{(RED)}$$

$$H_2PD(_{RED)} \rightarrow PD_{(OX)} + 2e^- + 2H^+$$

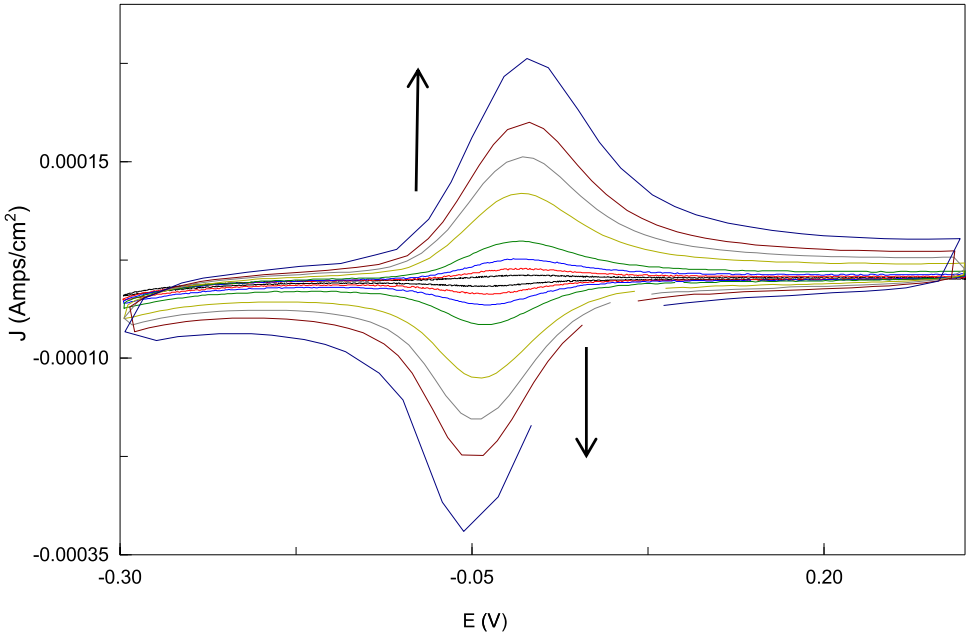

Fig. 5. Scan rate study showing CV of 0.1 M PB (pH 6.0) at GCE/LOx/pPD; potential range −0.3 V to 0.3 V vs. Ag/AgCl with scan rate (2- 300 mVs^{-1}).

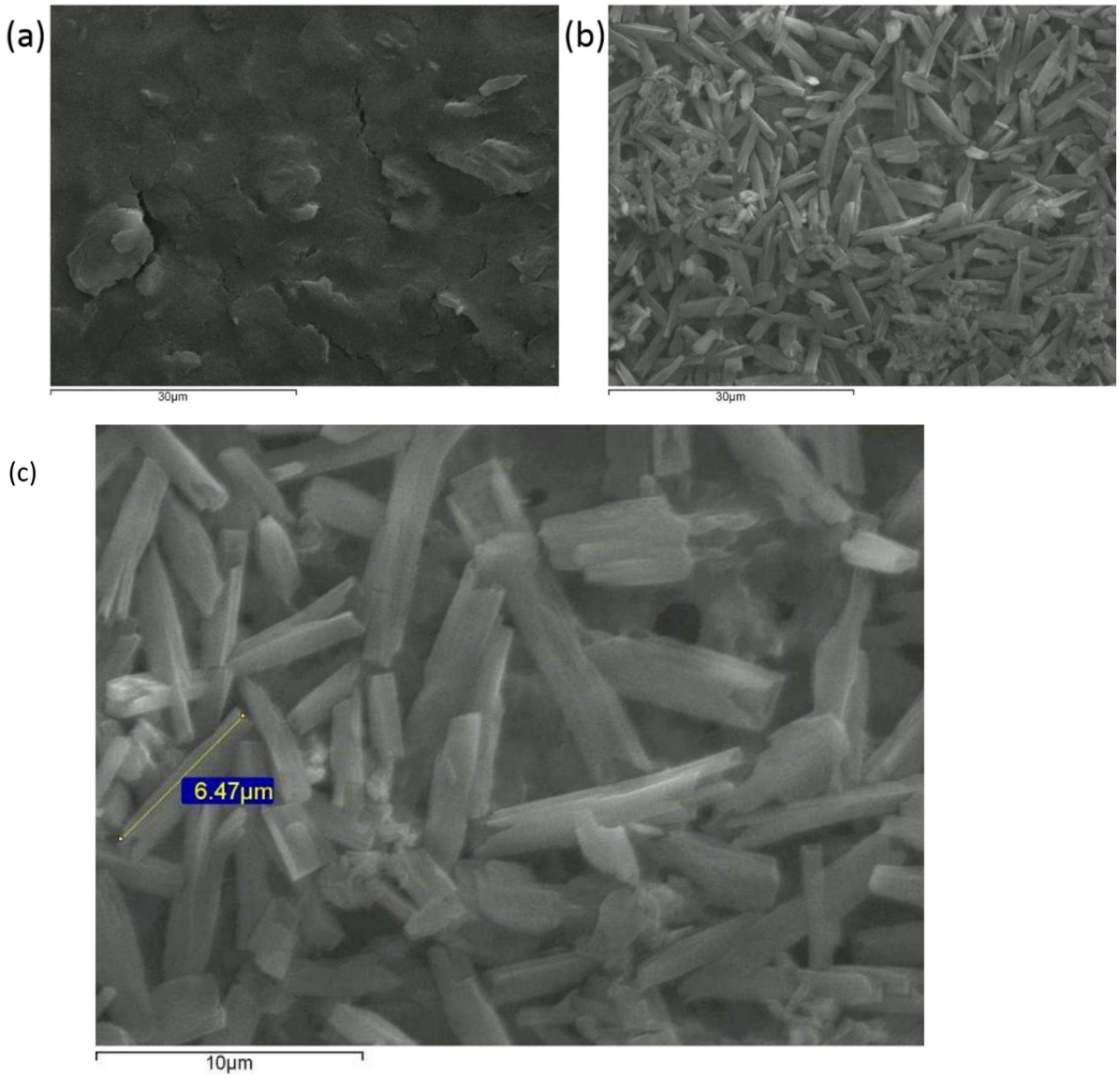

Fig. 6. SEM image of (a) Bare SPE (b) SPE/GInk/LOx/pPD and (c) SEM image of SPE/GInk/LOx/pPD.

Chronocoulometry was performed to study the relationship between charge and concentration at the oxidation peak (E_{app} = 0.12 V vs. Ag/AgCl). Fig. 9(b) shows the CC response to lactate concentrations (0.74 mM to 2.44 mM) at the GCE/GInk/LOx/pPD with corresponding calibration curve shown in Fig. 9 (c)) resulting in linear range 0.74 – 2.44×10^{-3} M, sensitivity 4.11×10^{-4}C $cm^{-2}mM^{-1}$, LOD of 0.06 mM and LOQ of 0.19 mM. The results of the calibration of GCE/GInk/LOx/pPD *via* CC analysis showed that operating at the oxidation potential of the

Table 1
Comparison of analytical performance for lactate biosensors (lactate oxidase).

	Linear Range (M)	Sensitivity	LOD (mM)	LOQ (mM)	Reference
LOx on N,N'-Bis(3,4-dihydroxybenzylidene)-1,2-diaminobenzene Schiff base tetradentate ligand-modified gold nanoparticles (3,4DHS–AuNPs)	Up to 8 x 10^{-4}	5.1 +/- 0.1 $\mu A\ mM^{-1}$	2.6 x 10^{-3}	8.6 x10^{-3}	[5]
LOx/solgel at Prussian blue modified electrode	5×10^{-7} – 1×10^{-3}	0.18 A M^{-1}	–	–	[21]
Copper metallic framework	0.7×10^{-6} – 1×10^{-3}	14.65 $\mu A\ mM^{-1}$	7.5 x10^{-4}		[8]
LOx at laponite/chitosan hydrogels	1×10^{-5} – 7×10^{-5}	0.326 A cm^{-2} M^{-1}	3.8 x10^{-3}	–	[22]
Pt/Chit/LOx/Chit/GA (direct H_2O_2 detection)	9.9 x 10^{-4} – 3.96 x 10^{-3}	6.64 x 10^{-4} C cm^{-2} mM^{-1}	0.43	1.44	This work
GCE/Chit/LOx/Chit/GA (5 mM $K_3Fe(CN)_6$)	9.9 x 10^{-4} – 5.66 x 10^{-3}	1.44 x 10^{-3} C $cm^{-2}mM^{-1}$	0.54	1.81	This work
GCE/GInk/LOx/PD reagentless with operation at E_{app} = 0.12 V vs. Ag/AgCl	7.4 x 10^{-4} – 2.44 x 10^{-3}	4.11 x 10^{-4} C cm^{-2} mM^{-1}	0.06	0.19	This work

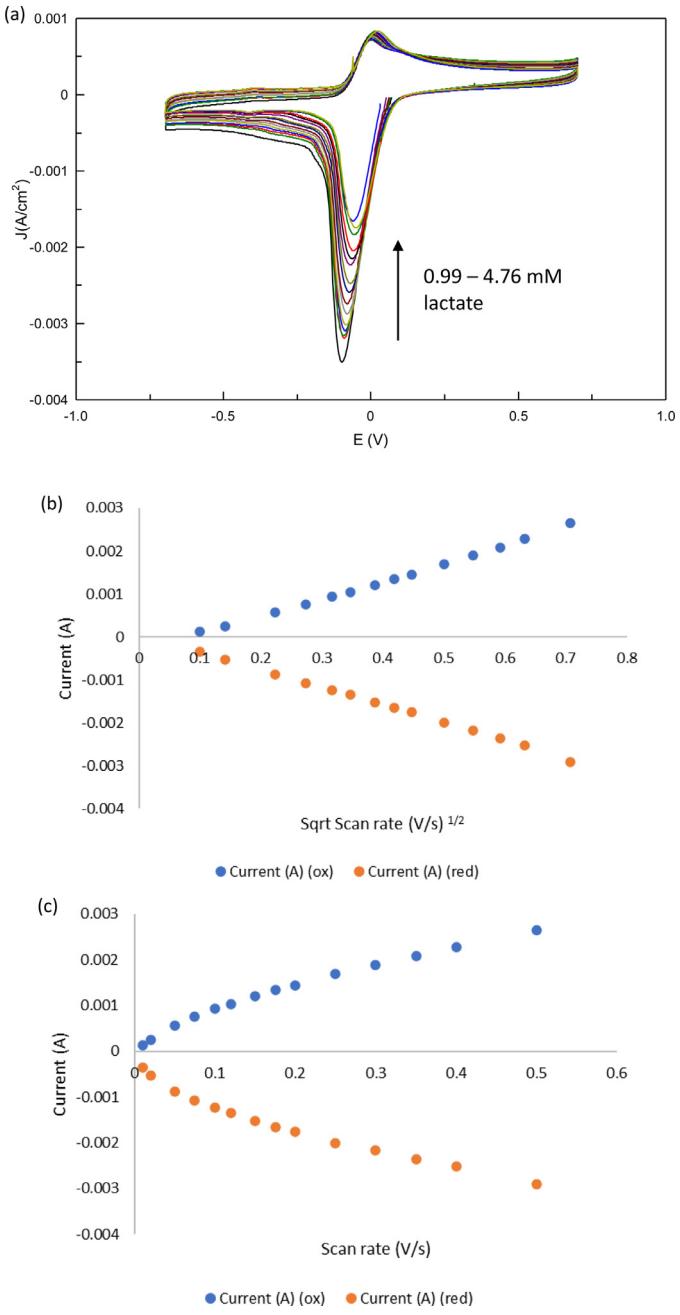

Fig. 7. (a) Enzymatic polymerisation using potential sweeping at a GCE/GInk/LOx electrode in 5 mM PD with lactate additions (0–4.76 mM) - potential range −0.7 V to 0.7 V vs. Ag/AgCl at 20 mVs^{-1}. pPD film studies - data plots of (b) I_{pa} and I_{pc} vs. ν (c) I_{pa} and I_{pc} vs. $\sqrt{\nu}$.

film, gave a greater linear range relative to the cathodic response E_{app} = −0.12 V vs. Ag/AgCl.

Table 1 provides a comparative study with respect to analytical performance of LOx based biosensors reported for use specifically in dairy/food analysis.

The optimal lactate biosensor which exploited the underlying graphite ink layer and the PD redox film resulted in good analytical performance and a relatively lower LOD/LOQ in comparison to prior iterations. A key advantage with this reagentless approach is capability to operate at low potential (0.12 V vs. Ag/AgCl) where signal selectivity can be achieved.

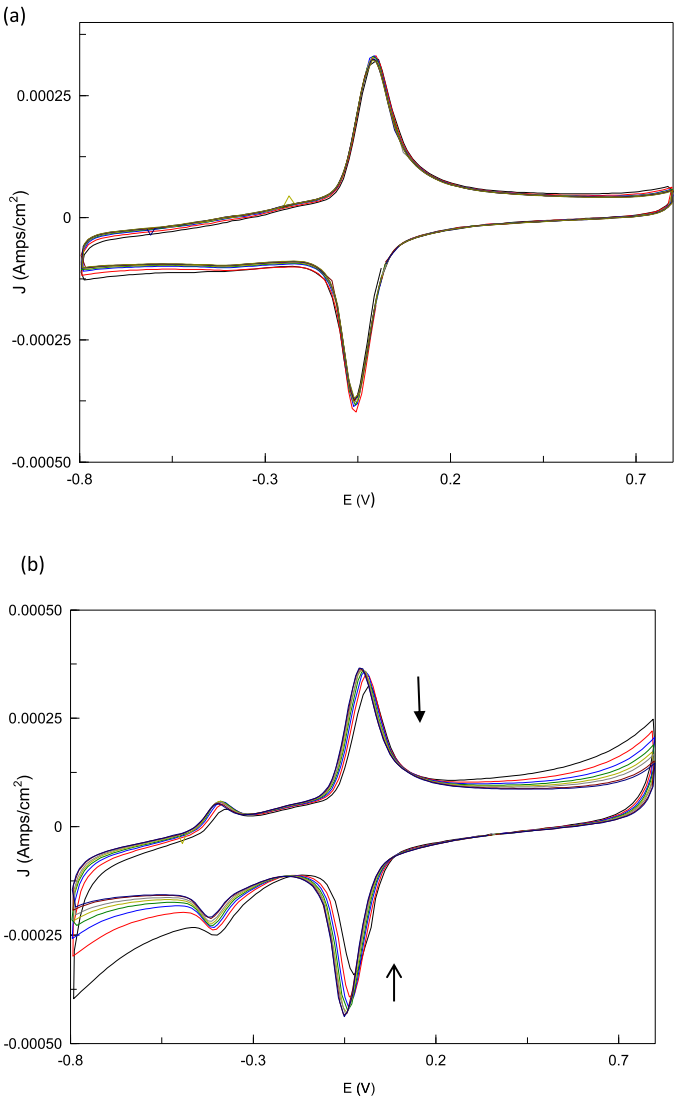

Fig. 8. Film stability studies at the pPD film formed at a GCE/GInk/LOx in pH 6 (A) and pH 4 (B), potential range −0.7 V to 0.7 V vs. Ag/ AgCl at 100 mVs^{-1} (20 cycles).

4. Conclusion

The work advances lactate sensing via a novel surface confined mediator, encapsulated at carbon based enzyme electrodes with surface enhanced properties driven by an underlying biocompatible graphite ink film. Attractive and novel properties of this approach included controlled deposition of PD via *in situ* generation of hydrogen peroxide which acted as an oxidant for film formation. The surface confined mediator responded to lactate additions at 0.12 V vs. Ag/AgCl and film properties were examined using voltammetric and surface techniques. The use of SEM and scanning electrochemical microscopy (SECM redox competition mode) provided surface topographical and imaging/enzyme reactivity information respectively.

Comparative studies indicated that the presence of the graphite ink improved the reversibility of the PD redox active film and provided a greater surface area for layer-by-layer modification. In the absence of GInk, pPD films exhibited ΔEp 0.109 V with $E_{1/2}$ −0.015 V, while with the GInk underlying layer ΔEp was 0.072 V with a slight cathodic shift in $E_{1/2}$ to −0.027 V. The redox film resulted in $E_{1/2}$ = 0.0284 V in pH 6

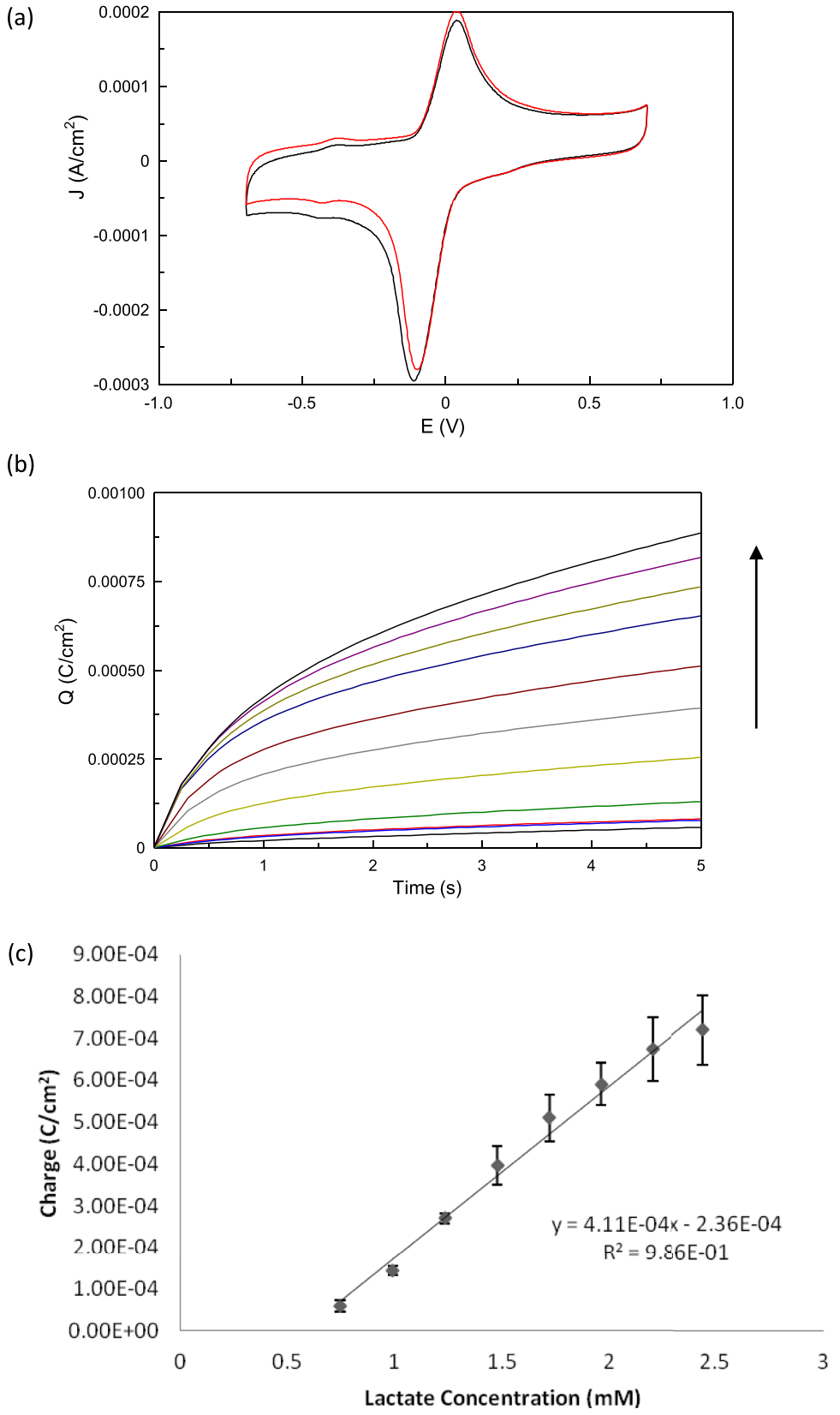

Fig. 9. (a) CV of 0.1 M PB (pH 6.0) (black line) and 0.99 mM lactate (red line) at a GCE/GInk/LOx/pPD. Potential range −0.7 to 0.7 V vs. Ag/AgCl at 100 mVs^{-1}. (b) CC response to lactate additions (0.74–2.44 mM) at a GCE/GInk//LOx/pPD electrode (E_{app} = 0.12 V vs. Ag/AgCl for 5 s). (C) Calibration plot of charge density vs. lactate concentration (0 – 2.44 mM) (n = 3).

electrolyte and $E_{1/2}$ = 0.0854 V in pH 4, confirming the pH dependant process ($2e^- 2H^+$). The resulting optimal biosensor responded to lactate over the range 0.74 – 2.44×10^{-3} M, with sensitivity of 4.11×10^{-4}C cm^{-2} mM^{-1}, LOD of 0.06 mM and LOQ of 0.19 mM comparing favourably with current literature. Transfer to screen printed electrodes for rapid analysis in agri-food applications forms the next stage of the work.

Declaration of Competing Interest

I can declare that there is no conflict of interest in this work.

Acknowledgements

The authors would like to acknowledge funding under Irish Research Council, EBP/2017/482.

Supplementary materials

Supplementary material associated with this article can be found, in the online version, at doi:10.1016/j.snr.2021.100032.

References

1 H. Cunha-Silva, MJ Arcos-Martinez, Dual range lactate oxidase-based screen printed amperometric biosensor for analysis of lactate in diversified samples, Talanta 188 (2018) 779–787, doi: 10.1016/j.talanta.2018.06.054.
2 C.S. Pundir, V. Narwal, B. Batra, Determination of lactic acid with special emphasis on biosensing methods: a review, Biosens. Bioelectron. 86 (2016) 777–790, doi: 10.1016/j.bios.2016.07.076.
3 I. Taurino, R. Reiss, M. Richter, M. Fairhead, L. Thony-Meyer, G. De Micheli, S. Carrara, Comparative study of three lactate oxidases from Aerococcus viridans for biosensing applications, Electrochima Acta 93 (2013) 72–79, doi: 10.1016/j.electacta.2013.01.080.
4 J. Di, J. Cheng, Q. Xu, H. Zheng, J. Zhuang, Y. Sun, K. Wang, X. Mo, S Bi, Direct electrochemistry of lactate dehydrogenase immobilized on silica sol-gel modified gold electrode and its application, Biosens. Bioelectron. 23 (5) (2007) 682–687, doi: 10.1016/j.bios.2007.08.002.
5 I. Bravo, M. Revenga-Parra, F. Pariente, E. Lorenzo, Reagent-less and robust biosensor for direct determination of lactate in food samples, Sens. Switzerl. 17 (1) (2017) 1–11, doi: 10.3390/s17010144.
6 I. Taurino, R. Reiss, M. Richter, M. Fairhead, L. Thony-Meyer, G. De Micheli, S. Carrara, Comparative study of three lactate oxidases from Aerococcus viridans for biosensing applications, Electrochim. Acta 93 (2013) 72–79, doi: 10.1016/j.electacta.2013.01.080.
7 A.M. Herrero, T. Requena, A.J. Reviejo, J.M. Pingarrón, Determination of L-lactic acid in yoghurt by a bienzyme amperometric graphite-Teflon composite biosensor, Eur. Food Res. Technol. 219 (5) (2004) 556–559, doi: 10.1007/s00217-004-0973-7.
8 H. Cunha-Silva, MJ Arcos-Martinez, Dual range lactate oxidase-based screen printed amperometric biosensor for analysis of lactate in diversified samples, Talanta 188 (2018) 779–787, doi: 10.1016/j.talanta.2018.06.054.
9 E. Zor, Y. Oztekin, L. Mikoliunaite, J. Voronovic, A. Ramanviciene, Z. Anusevicius, H. Bingol, A. Ramanavicius, 1,10-Phenanthroline-5,6-dione and 9,10-phenanthrenequinone as redox mediators for amperometric glucose biosensors, J. Solid State Electrochem. 18 (6) (2014) 1529–1536, doi: 10.1007/s10008-013-2368-9.
10 Y. Oztekin, V. Krikstolaityte, A. Ramanaviciene, Z. Yazicigil, A. Ramanavicius, 1,10-Phenanthroline derivatives as mediators for glucose oxidase, Biosens. Bioelectron. 26 (1) (2010) 267–270, doi: 10.1016/j.bios.2010.05.005.
11 H. Hadadzadeh, M.M. Olmstead, A.R. Rezvani, N. Safari, H. Saravani, Synthesis, structure, spectroscopic, magnetic and electrochemical studies of NiII phen-dione complex, Inorg. Chim. Acta 359 (7) (2006) 2154–2158, doi: 10.1016/j.ica.2006.02.015.
12 K. Yokoyama, A. Wakabayashi, K. Noguchi, N. Nakamura, H. Ohno, Structure and spectroelectrochemical property of a ruthenium complex containing phenanthroline-quinone, and assembly of the complexes on a gold electrode, Inorg. Chim. Acta 359 (3) (2006) 807–814, doi: 10.1016/j.ica.2005.05.038.
13 M. Hedenmo, A. Narváez, E. Domínguez, I. Katakis, Reagentless amperometric glucose dehydrogenase biosensor based on electrocatalytic oxidation of NADH by osmium phenanthrolinedione mediator, Analyst 121 (12) (1996) 1891–1895, doi: 10.1039/an9962101891.
14 H. Ciftci, Y. Oztekin, U. Tamer, A. Ramanaviciene, A. Ramanavicius, Electrochemical biosensor based on glucose oxidase encapsulated within enzymatically synthesized poly(1,10-phenanthroline-5,6-dione), Colloids Surf. B Biointerf. 123 (2014) 685–691, doi: 10.1016/j.colsurfb.2014.10.032.
15 A.J. Bandodkar, W. Jia, J. Ramírez, J. Wang, Biocompatible enzymatic roller pens for direct writing of biocatalytic materials: "do-it-yourself" electrochemical biosensors, Adv. Healthc. Mater. 4 (8) (2015) 1215–1224, doi: 10.1002/adhm.201400808.
16 C.G. Zoski, Review—advances in scanning electrochemical microscopy (SECM), J. Electrochem. Soc. 163 (4) (2016) H3088–H3100, doi: 10.1149/2.0141604jes.
17 Mirkin M.V. Horrocks B.R., Electroanalytical measurements using the scanning electrochemical microscope. 2000;406:119–146. https://doi.org/10.1016/S0003-2670(99)00630-3
18 I. Morkvenaite-Vilkonciene, A. Ramanaviciene, P. Genys, A. Ramanavicius, Evaluation of enzymatic kinetics of GOx-based electrodes by scanning electrochemical microscopy at redox competition mode, Electroanalysis 29 (6) (2017) 1532–1542, doi: 10.1002/elan.201700022.
19 A.O. Okunola, T.C. Nagaiah, X. Chen, K. Eckhard, W. Schuhmann, M. Bron, Visualization of local electrocatalytic activity of metalloporphyrins towards oxygen reduction by means of redox competition scanning electrochemical microscopy (RC-SECM), Electrochim. Acta 54 (22) (2009) 4971–4978, doi: 10.1016/j.electacta.2009.02.047.
20 M. Wu, X. Mao, X. Li, X. Yang, L. Zhu, 1,10 phenanthroline-5,6-dione adsorbed on carbon nanotubes: the electchemicstry and catalytic oxidation of ascorbic acid, J. Electroanal. Chem. 682 (1–6) (2012), doi: 10.1016/j.jelechem.2012.06.007.
21 E.I. Yashina, A.V. Borisova, E.E. Karyakina, V.M.Y. Shchegolikhina, D.A. Sakharov, A.G. Tonevitsky, A.A Karyakin, Sol-gel immobilization of lactate oxidase from organic solvent: toward the advanced lactate biosensor, Anal. Chem. 82 (2021) 1601–1604, doi: 10.1021/ac9027615.
22 V.P. Zanini, B. Loez de Mishima, V. Solis, An amperometric biosensor based on lactate oxidase immobilized in laponite–chitosan hydrogel on a glassy carbon electrode. Application to the analysis of L-lactate in food samples, Sens. Actuators B 155 (2011) 75–80, doi: 10.1016/j.snb.2010.11.026.